


Deterministic realization of trace-preserving channels in linear-optical systems

Xiang Zhan^{1,2}, Dengke Qu,³ and Peng Xue^{3,*}

¹*School of Science, Nanjing University of Science and Technology, Nanjing 210094, China*

²*MIT Key Laboratory of Semiconductor Microstructure and Quantum Sensing, Nanjing University of Science and Technology, Nanjing 210094, China*

³*Beijing Computational Science Research Center, Beijing 100084, China*

 (Received 9 May 2022; revised 31 July 2022; accepted 8 September 2023; published 20 September 2023)

A quantum channel describes the general evolution of quantum systems, which is therefore a critical issue for quantum simulation and a fundamental element of quantum information. To realize quantum channels, an efficient method is to randomly implement Kraus operators, which does not require any ancillary quantum system. For open systems, it is natural to extend the method from implementation of unitary Kraus operators to nonunitary ones. However, when some Kraus operators are not proportional to unitary ones, this method becomes probabilistic even if the channel is trace preserving. In this paper, to overcome this drawback, we propose an algorithm to deterministically realize arbitrary trace-preserving channels with only one ancillary qubit and finite iterations of evolutions of the combined states of the system and the ancilla. Moreover, to show the validity of the method, we experimentally realize conventional and modified Landau–Streater channels based on the algorithm. Our results shed light on quantum simulation of quantum channels for open systems.

DOI: [10.1103/PhysRevA.108.032611](https://doi.org/10.1103/PhysRevA.108.032611)

I. INTRODUCTION

Quantum simulation promises to be a near-term application of quantum information science and technology [1–5]. This is because it focuses on simulating specific classically intractable systems and thereby significantly reduces the onerous requirements of universal quantum computation. Therefore, it is a pursuit encoded in the genes of quantum simulation to reduce the use of quantum resources. When simulating an open quantum system, the pursuit naturally becomes using a smaller quantum system to act as its environment. The dynamics of an open quantum system can be described by a quantum channel [6], which is a mapping of quantum systems from an initial state ρ to a final state ρ' , i.e., $\mathcal{E} : \rho \mapsto \rho'$. In this paper, we consider the important issue of efficiently realizing a general quantum channel, which plays a key role in quantum information processing [6–13].

A straightforward method to realize quantum channels is to embed the system into a larger closed system and then implement unitary transformations to the whole system [14]. Many attempts in this area are to reduce the number or dimension of the ancillary quantum systems [15,16]. Among these, an efficient and widely used method is based on Kraus representation of the quantum channel, which does not require any ancillary quantum system [17–23].

A quantum channel \mathcal{E} is described in the Kraus representation as

$$\mathcal{E}[\rho] = \sum_{i=1}^r K_i \rho K_i^\dagger, \quad (1)$$

where $\{K_i\}$ are Kraus operators and the minimal number of r is the Kraus rank of the channel. With this notation, the final state of a channel is a mixture of states $K_i \rho K_i^\dagger / \text{Tr}[K_i \rho K_i^\dagger]$ with probabilities $\text{Tr}[K_i \rho K_i^\dagger]$. For the trace-preserving channel (TC), these probabilities satisfy $\sum_{i=1}^r \text{Tr}[K_i \rho K_i^\dagger] = 1$. A special case of TC is the trace-preserving random-unitary channel (TRC), of which all Kraus operators are proportional to unitary ones as $K_i = \sqrt{p_i} \bar{K}_i$ with $\bar{K}_i \bar{K}_i^\dagger = \mathbb{1}$. For TRC, the probabilities p_i are independent of the initial state and satisfy $\sum_{i=1}^r p_i = 1$. Therefore, these channels can be deterministically realized by randomly implementing unitary operations $\bar{K}_i = K_i / \sqrt{p_i}$ [see Fig. 1(a)].

Generally, a TC may have some Kraus operators that are not proportional to any unitary operator, which we termed as a trace-preserving but not random-unitary channel (TNRC). To realize a TNRC, it is still possible to use the efficient method above by randomly implementing operations $\bar{K}_i = K_i / \sqrt{q_i}$ with probabilities p_i [24–26]. Physically implementable operations \bar{K}_i should satisfy $\bar{K}_i \bar{K}_i^\dagger \leq \mathbb{1}$ [27–32], where the equality holds when and only when \bar{K}_i is unitary. For TNRC, some of the operations \bar{K}_i must be nonunitary, which result in $\text{Tr}[\bar{K}_i \rho \bar{K}_i^\dagger] < 1$. Therefore, implementing these nonunitary operations could result in the loss of the system [24–26]. Formally, the final state of the realized channel is $\sum_{i=1}^r p_i \bar{K}_i \rho \bar{K}_i^\dagger$, of which the trace is $\sum_{i=1}^r p_i \text{Tr}[\bar{K}_i \rho \bar{K}_i^\dagger] < \sum_{i=1}^r p_i = 1$. Note that this trace corresponds to the probability of obtaining a final state for a given initial state. Therefore, the realized channel is not a TC but a probabilistic simulation of the TC [24–26]. To deterministically realize a TC, this probability should be one.

The basic idea to efficiently and deterministically realize arbitrary TC was first pointed out by Lloyd and Viola

*gnep.eux@gmail.com

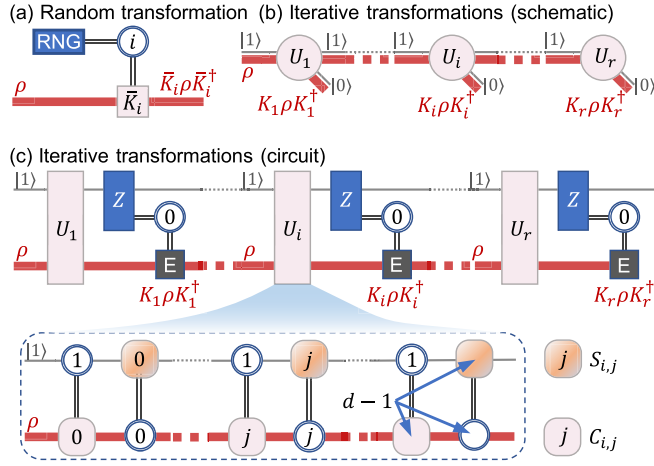


FIG. 1. (a) Schematic for realizing quantum channels via randomly implementing the operation \bar{K}_i determined by a random number generator (RNG). (b) Schematic of our method to implement quantum channels, which uses an ancillary qubit initialized in state $|1\rangle$ and iteratively implements unitary transformations U_i to the composite system. After each U_i , the ancillary qubit is measured by Pauli Z (not shown). If the outcome is 0, finish the process; otherwise, the outcome is 1, the ancillary qubit collapses to state $|1\rangle$, and the composite system moves to the next iteration. (c) Circuit for our method, where the process ends (denoted by the black rectangle) once the measurement outcome is 0. The inset shows the circuit for each unitary transformation U_i .

(LV) [33], which we termed the LV method. In the LV method, arbitrary TC can be realized by channels with Kraus rank of 2 in an adaptive fashion. A channel with Kraus rank of 2 can be efficiently realized using the traditional method of enlarging the system with an ancillary qubit [34,35]. The ancillary qubit is initialized in state $|1\rangle$ and then a unitary operation U is implemented to the composite system. After tracing out the ancillary qubit, the final state of the system is $\langle 0|U(|1\rangle\langle 1| \otimes \rho)U^\dagger|0\rangle + \langle 1|U(|1\rangle\langle 1| \otimes \rho)U^\dagger|1\rangle$, which is equivalent to the result of a channel with two Kraus operators $\langle 0|U|1\rangle$ and $\langle 1|U|1\rangle$.

Shen *et al.* [36] proposed an explicit form of the LV method based on a binary-tree construction scheme for realizing positive operator-valued measurement (POVM) [37]. In this method, an ancillary qubit is introduced and a unitary transformation on the composite system followed by a measurement on the qubit is iteratively applied. In each iteration, the outcome is fed back to control the unitary operation of the next iteration. As a result, the binary outcomes create a binary tree composed of unitary operations. Therefore, we term this method the tree LV method.

In this paper, we propose and experimentally demonstrate another explicit form of the LV method. Our protocol also introduces an ancillary qubit and iteratively applies a unitary transformation on the composite system followed by a measurement on the qubit. The key difference is that the two possible outcomes of the measurement determine whether to apply the next iteration or to end the process. As illustrated in Fig. 1(b), our protocol creates a path graph composed of unitary operations, which we termed as the path LV method.

Importantly, our method incorporates the realization of specific unitary operators and is presented in an algorithmic manner, making it highly convenient to use. We experimentally demonstrate the application of our method in linear optical systems.

This paper is organized as follows. In Sec. II, we introduce our general protocol for realizing arbitrary TC. Section III provides examples. In Sec. IV, we present our experimental setup for realizing these example channels. The experimental results are provided in Sec. V. Finally, we summarize and discuss our results in Sec. VI.

II. PROPOSAL

A. Basic idea

Following the ideas in Refs. [33,36], our basic idea to realize a TC is illustrated in Figs. 1(b) and 1(c). We introduce an ancillary qubit initialized at state $|1\rangle$ and iteratively implement unitary operation U_i . After each U_i , we measure the ancillary qubit by Z in the basis $\{|0\rangle\langle 0|, |1\rangle\langle 1|\}$. If the outcome is 0, we terminate the process; otherwise, we enter the next iteration. Therefore, our protocol defines a path graph composed of unitary operations, as shown in Fig. 1(b).

Let us first consider the action of each iteration. We consider that the process moves to the next iteration only when the measurement outcome is 1. In this case, the ancillary qubit collapses to the state $|1\rangle$. Therefore, each iteration i begins with the composite system at state $|1\rangle\langle 1| \otimes \rho_{i-1}$. In this iteration, the unitary operation U_i transforms the state into $U_i(|1\rangle\langle 1| \otimes \rho_{i-1})U_i^\dagger$. Therefore, the measurement outcome is 0 or 1 with probability $\text{Tr}[K'_i \rho_{i-1} K_i'^\dagger]$ or $\text{Tr}[L'_i \rho_{i-1} L_i'^\dagger]$, respectively, where $K'_i = \langle 0|U_i|1\rangle$ and $L'_i = \langle 1|U_i|1\rangle$. Moreover, when the outcome is 0, the process terminates and generates a final state $K'_i \rho_{i-1} K_i'^\dagger / \text{Tr}[K'_i \rho_{i-1} K_i'^\dagger]$; when the outcome is 1, the process moves to the next iteration with the composite system at state $|1\rangle\langle 1| \otimes \rho_i = |1\rangle\langle 1| \otimes L'_i \rho_{i-1} L_i'^\dagger / \text{Tr}[L'_i \rho_{i-1} L_i'^\dagger]$.

Let us analyze the channel generated by this process. The process terminates after iteration i when the measurement outcome is 0 and all previous outcomes are 1. Therefore, it terminates after first iteration with a probability $\text{Tr}[K'_1 \rho_0 K_1'^\dagger] = \text{Tr}[K_1 \rho_0 K_1^\dagger]$ or after iteration $i \geq 2$ with a probability

$$\begin{aligned} & \text{Tr}[K'_i \rho_{i-1} K_i'^\dagger] \prod_{i'=1}^{i-1} \text{Tr}[L'_{i'} \rho_{i'-1} L_{i'}'^\dagger] \\ &= \text{Tr} \left[K'_i \left(\prod_{i'=i-1}^1 L'_{i'} \right) \rho_0 \left(\prod_{i'=1}^{i-1} L'_{i'} \right) K_i'^\dagger \right] \\ &= \text{Tr}[K_i \rho_0 K_i^\dagger], \end{aligned} \quad (2)$$

where $K_i = K'_i (\prod_{i'=i-1}^1 L'_{i'})$. Moreover, when the process terminates after iteration i , the final state is $K'_i \rho_{i-1} K_i'^\dagger / \text{Tr}[K'_i \rho_{i-1} K_i'^\dagger] = K_i \rho_0 K_i^\dagger$. Hence such a process realizes a channel that transforms state ρ_0 into $K_i \rho_0 K_i^\dagger$ with probability $\text{Tr}[K_i \rho_0 K_i^\dagger]$. The crucial task is designing specific unitary operations to let the operations K_i be desired ones.

A critical issue with our method is that the process appears to be probabilistic since the termination condition depends on the measurement outcomes. However, when the unitary

operations are properly chosen to realize a channel with Kraus rank of r , the process terminates and generates a final state within r iterations with a probability of $\sum_{i=1}^r \text{Tr}[K_i \rho_0 K_i^\dagger]$. Therefore, when the desired channel is a TC, which ensures $\sum_{i=1}^r \text{Tr}[K_i \rho_0 K_i^\dagger] = 1$ for arbitrary state ρ_0 , the process deterministically yields a final state. We will further demonstrate this determinism by showing that the measurement outcome of the r th iteration must be 0. In this case, the final transformation must be a tensor product of σ_x on the ancillary qubit and a unitary transformation of the d -dimensional system.

The tree LV method has a significant advantage in terms of the required number of iterations, i.e., the level of the tree [36]. A tree with level l can realize a channel with Kraus rank 2^l . In this case, it is necessary to determine $2^l - 1$ unitary operations, which is similar to our method that requires 2^l unitary operations. It is worth mentioning that the choice of a method should take into account the noise of the experimental system.

Let us consider a simple case where each unitary transformation U is followed by a general Pauli channel as $\mathcal{P}(\rho) = \sum_{j=0}^{d^2-1} p_j \sigma_j \rho \sigma_j^\dagger$, where $\sum_{j=0}^{d^2-1} p_j = 1$ and σ_j are Pauli operators of the d -dimensional system with σ_0 being the identity. In this case, the noise strength is $\epsilon = 1 - p_0$. We have simulated the effect of this noise on the realized channels with Kraus rank 16 of a four-dimensional system. Specifically, we randomly generate unitary transformations in a method and obtain a channel \mathcal{E} as the ideal one. For each case, we obtain the noisy channel $\tilde{\mathcal{E}}$ for specific noise ϵ by randomly generating p_j for $j = 1, \dots, 16$ and then normalizing these to $\epsilon p_j / \sum_{j=1}^{16} p_j$.

To compare the noise channel with the ideal one, we adopt the Choi-Jamiołkowski representation [38,39] of a quantum channel as

$$\Upsilon_{\mathcal{E}} = \mathcal{E} \otimes \mathcal{I}[|I\rangle\langle I|], \quad (3)$$

where $|I\rangle = \sum_{k=0}^{d-1} |kk\rangle$ is an unnormalized maximally entangled state. With this representation, the action of channel is $\mathcal{E}[\rho] = \text{Tr}_2[(\mathbb{1}_d \otimes \rho^T) \Upsilon_{\mathcal{E}}]$, where Tr_2 denotes the partial trace on the second d -dimensional system. It is to be noted that the Choi matrix $\Upsilon_{\mathcal{E}}$ satisfies the same constraints as a density matrix [40]. Using Choi-Jamiołkowski representation of quantum channels, the fidelity between two channels \mathcal{E}_1 and \mathcal{E}_2 can be measured by the state fidelity between the Choi matrices [41] as

$$\mathcal{F}(\Upsilon_{\mathcal{E}_1}, \Upsilon_{\mathcal{E}_2}) = \frac{1}{d} \text{Tr}[\sqrt{\sqrt{\Upsilon_{\mathcal{E}_1}} \Upsilon_{\mathcal{E}_2} \sqrt{\Upsilon_{\mathcal{E}_1}}}], \quad (4)$$

For each method, we have simulated 100 pairs of ideal and noisy channels and calculated their fidelities for each ϵ . As shown in Fig. 2, the path LV method appears to exhibit greater robustness to small noise.

B. Specific protocol

Let us introduce our protocol for realizing arbitrary TC using the iterative idea described above. Moreover, our protocol designs the unitary operations in an iterative manner, as shown in Fig. 1(d). Therefore, our protocol includes two iterative loops in total.

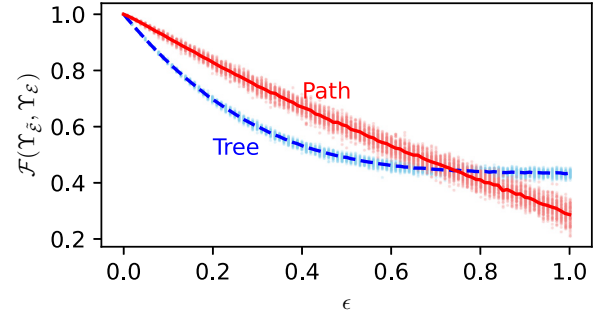


FIG. 2. Fidelities between a random channel \mathcal{E} and its noisy version $\tilde{\mathcal{E}}$ due to each unitary transformation suffering from a general Pauli noise with strength ϵ . The scatter plots represent the results for the tree LV method (blue dashed) or the path LV method (red solid) and the corresponding lines show their average values.

To describe our protocol, we denote the Kraus operators as $K_i = \sum_{j=0}^{d-1} |j\rangle\langle\psi_{i,j}|$, where $|\psi_{i,j}\rangle$ are unnormalized states and their normalized forms are $|\tilde{\psi}_{i,j}\rangle = |\psi_{i,j}\rangle / \|\psi_{i,j}\|$. It is worth mentioning that a Kraus operator K_i is proportional to a unitary operator if and only if states $|\psi_{i,j}\rangle$ are mutually orthogonal and their norms $\|\psi_{i,j}\|$ are equal. With this notation, our method works as follows.

(i) Initialize the ancillary qubit in the state $|1\rangle$ and set iteration numbers as $(i, j) = (1, 0)$.

(ii) Implement the unitary operation $B_{i,j} A_{i,j}$ to the composite system, where $A_{i,j}$ and $B_{i,j}$ will be introduced below.

(iii) If $j < d - 1$, update $j = j + 1$ and repeat step (ii); otherwise, move to step (iv).

(iv) Measure the ancillary qubit in the basis $\{|0\rangle\langle 0|, |1\rangle\langle 1|\}$. If the outcome is 0, finish the process; otherwise, set $i = i + 1$ and $j = 0$ and then repeat step (ii).

The unitary operations in step (ii) are ancilla-control-system A_{ij} and system-control-ancilla operations $B_{i,j}$, respectively, i.e.,

$$\begin{aligned} A_{i,j} &= |1\rangle\langle 1| \otimes C_{i,j} + |0\rangle\langle 0| \otimes \mathbb{1}, \\ B_{i,j} &= S_{i,j} \otimes |j\rangle\langle j| + \mathbb{1} \otimes (\mathbb{1} - |j\rangle\langle j|), \end{aligned} \quad (5)$$

where $S_{i,j} = (r_{i,j} \sigma_x - t_{i,j} \sigma_z)$ is a single-qubit operation. The unitary operations $C_{i,j}$ are chosen to satisfy

$$\langle j| C_{i,j} = \frac{\langle \tilde{\psi}_{i,j} | L_{i,j-1}^+}{\|\langle \tilde{\psi}_{i,j} | L_{i,j-1}^+ \|^+}, \quad (6)$$

where the superscript $+$ denotes Moore-Penrose inverse [42], and the real parameters $r_{i,j}$ and $t_{i,j}$ are determined as

$$\begin{aligned} r_{i,j} &= \|\psi_{i,j}\| \times \|\langle \tilde{\psi}_{i,j} | L_{i,j-1}^+ \|^+, \\ t_{i,j} &= \sqrt{1 - r_{i,j}^2}. \end{aligned} \quad (7)$$

The operators $L_{i,j}$ are recursively defined as

$$L_{i,j} = [\mathbb{1} - (1 - t_{i,j})|j\rangle\langle j|] C_{i,j} L_{i,j-1},$$

with $L_{1,-1} = \mathbb{1}$ and $L_{i,-1} = L_{i-1,d-1}$. Note that there is only one restriction of the j th row to the choice of $C_{i,j}$. Therefore, the choice of $C_{i,j}$ can be adjusted according to the features of a specific experimental system.

C. Proof of the protocol

Now, let us show how this procedure deterministically realizes the desired channel. After step (ii) of the procedure, the state of the composite system is $|\Psi_{i,j}\rangle / \|\Psi_{i,j}\|$, where

$$|\Psi_{i,j}\rangle = |0\rangle \otimes \sum_{l=0}^j r_{i,l} \langle l | C_{i,l} L_{i,l-1} |\psi\rangle |l\rangle + |1\rangle \otimes L_{i,j} |\psi\rangle. \quad (8)$$

Therefore, if the outcome is 0 in step (iv), the state of the system undergoes a transformation as

$$\begin{aligned} T_i &= \sum_{l=0}^{d-1} r_{i,l} |l\rangle \langle l | C_{i,l} L_{i,l-1} \\ &= \sum_{l=0}^{d-1} \frac{r_{i,l}}{\|\langle \tilde{\psi}_{i,j} | L_{i,j-1}^+ \rangle\|} |l\rangle \langle \tilde{\psi}_{i,j} | L_{i,j-1}^+ \\ &= \sum_{l=0}^{d-1} |l\rangle \langle \psi_{i,l} | = K_i. \end{aligned} \quad (9)$$

Here the second equality is due to the choice of $C_{i,j}$ in Eq. (6) and the third equality is due to the choice of $r_{i,j}$ in Eq. (7) and a condition (C1) $|\tilde{\psi}_{i,l}\rangle \in \text{supp}(L_{i,j-1}^+) = \text{supp}(L_{i,j-1})$.

We now show the condition (C1) and another one (C2) $r_{i,j} \leq 1$, which ensures the process being a well-defined one. Given a TC with Kraus operators $K_i = \sum_{j=0}^{d-1} |j\rangle \langle \psi_{i,j}|$, one can construct a POVM with elements $|\psi_{i,j}\rangle \langle \psi_{i,j}|$ [43]. This POVM satisfies $\sum_{\text{all}} |\psi_{i,j}\rangle \langle \psi_{i,j}| = \sum_{<} |\psi_{k,l}\rangle \langle \psi_{k,l}| + L_{i,j} L_{i,j}^\dagger = \mathbb{1}$, where \sum_{all} denotes summation over all $i \in \{1, \dots, r\}$ and $j \in \{0, \dots, d-1\}$ and $\sum_{<}$ is over $k < i$ with $l \in \{0, \dots, d-1\}$ and $k = i$ with $l < j$. Thus we have $|\tilde{\psi}_{i,l}\rangle \in \text{supp}(L_{i,j-1})$ and $r_{i,j}^2 = \|\psi_{i,j}\|^2 \times \|\langle \tilde{\psi}_{i,j} | L_{i,j-1}^+ \rangle\| \leq 1$. That is, Eq. (9) holds and the process is well defined.

According to the above, the process ends with state $K_i |\psi\rangle / \|K_i |\psi\rangle\|$ if the measurement outcome at step (iv) is 0 with the iteration number $(i, d-1)$. In step (iv), the outcome is 0 with probability $P'_i = \|K_i |\psi\rangle\|^2 / \|\Psi_{i,d-1}\|^2 = 1 - \|L_{i,d-1} |\psi\rangle\|^2 / \|\Psi_{i,d-1}\|^2$. Since step (ii) only implements unitary operations to the system, it is obvious that $\|\Psi_{i,j}\| = \|L_{i-1} |\psi\rangle\|$. Therefore, for $i \geq 2$, we have $\|\Psi_{i,d-1}\|^2 = \|L_{i-1,d-1} |\psi\rangle\|^2 = (1 - P'_{i-1}) \|\Psi_{i-1,d-1}\|^2 = \|\Psi_{i-1,d-1}\|^2 - \|K_{i-1} |\psi\rangle\|^2 = \dots = \|\Psi_{1,d-1}\|^2 - \sum_{l=1}^{i-1} \|K_l |\psi\rangle\|^2$. Note that $\|\Psi_{1,d-1}\|^2 = 1$ and the trace preservation implies $\sum_{i=1}^r \|K_i |\psi\rangle\|^2 = 1$, so we have $\|\Psi_{i,d-1}\|^2 = \sum_{l=i}^r \|K_l |\psi\rangle\|^2$. Therefore, the probabilities satisfy $P'_i = \|K_i |\psi\rangle\|^2 / \sum_{l=i}^r \|K_l |\psi\rangle\|^2$.

Let us consider the probability P_i that the process ends with iteration number $(i, d-1)$. For $i = 1$, it is simply $P_1 = P'_1 = \|K_1 |\psi\rangle\|^2$. The process ends with iteration number $(i, d-1)$ only when outcomes of previous measurements are 1. Therefore, for $i > 1$, the probability is $P_i = P'_i \prod_{l=1}^{i-1} (1 - P'_l) = \frac{\|K_i |\psi\rangle\|^2}{\sum_{k=i}^r \|K_k |\psi\rangle\|^2} \prod_{l=1}^{i-1} \left(\frac{\sum_{k=l+1}^r \|K_k |\psi\rangle\|^2}{\sum_{k=l}^r \|K_k |\psi\rangle\|^2} \right) = \|K_i |\psi\rangle\|^2$. Hence the process successfully realizes the channel by output state $K_i |\psi\rangle / \|K_i |\psi\rangle\|$ with probability $\|K_i |\psi\rangle\|^2$.

In the last iteration with iteration number $(r, d-1)$, the probability of obtaining outcome 0 is $P'_r = \|\langle K_r |\psi\rangle\|^2 / \|\Psi_r |\psi\rangle\|^2 = 1$; that is, the outcome has to be 0. Hence our method is deterministic.

III. EXAMPLES: LANDAU-STREATER CHANNELS

As an example, we experimentally realize the Landau-Streater channel (LSC), which was originally proposed as an example of both unital channel (UC) and TNRC [44,45]. Here, a channel \mathcal{E} is UC if $\mathcal{E}[\mathbb{1}] = \mathbb{1}$. Therefore, all TRCs are UC but not vice versa, due to counterexamples as LSC.

The Kraus representation of LSC of the d -dimensional ($d \geq 3$) system is

$$\Phi_d[\rho] = \frac{4}{d^2 - 1} (J_x \rho J_x + J_y \rho J_y + J_z \rho J_z), \quad (10)$$

where J_x , J_y , and J_z are spin projection operators of spin- d particles. For qutrit ($d = 3$), the spin operators are

$$\begin{aligned} J_x &= (|0\rangle\langle 1| + |1\rangle\langle 0| + |1\rangle\langle 2| + |2\rangle\langle 1|) / \sqrt{2}, \\ J_y &= i(-|0\rangle\langle 1| + |1\rangle\langle 0| - |1\rangle\langle 2| + |2\rangle\langle 1|) / \sqrt{2}, \\ J_z &= |0\rangle\langle 0| - |2\rangle\langle 2|. \end{aligned} \quad (11)$$

For the qudit ($d = 4$), the operators are

$$\begin{aligned} J_\mu &= \sum_{j=0}^2 a_\mu \sqrt{\lambda_j \lambda_{j+1}} (|j\rangle\langle j+1| + b_\mu |j+1\rangle\langle j|), \\ J_z &= \sum_{j=0}^3 \lambda_j |j\rangle\langle j|, \end{aligned} \quad (12)$$

where $\mu = x, y$, $a_x = b_x = 1$, $a_y = i$, $b_y = -1$, $\lambda_0 = -\lambda_3 = 3/2$, and $\lambda_1 = -\lambda_2 = 1/2$.

Using our method, we can determine a choice of operations to realize these two channels (see the Appendixes). It is worth noting that, for all Kraus operators in the Φ_4 channel, interference happens within two subspaces spanned by $\{|0\rangle, |2\rangle\}$ and $\{|1\rangle, |3\rangle\}$. Moreover, using suitable phase-tuning and permutation operations, Kraus operators on these two subspaces can be identical. Therefore, we can simplify the procedure by simultaneously implementing operations on the two subspaces.

Different from TRC, there are TNRCs that are nonunital channels. A more interesting difference arises when applying different unitary transformations to Kraus operators. After the transformation, any TRC is still a TRC, which is still UC, but a TNRC that was a UC may become not a UC. For example, we consider a channel Φ'_3 with Kraus operators $U_u J_u$, where J_u are Kraus operators of Φ_3 , $U_u = \frac{1}{\sqrt{2}} (|0\rangle\langle 0| + c_u |0\rangle\langle 2| + |2\rangle\langle 0| - c_u |2\rangle\langle 2|) + |1\rangle\langle 1|$, with $c_x = -c_y = 1$ for $u = x, y$ and $U_z = \mathbb{1}$ (see the Appendixes).

IV. EXPERIMENTAL SETUP

A. Optical realization of our method

Let us first consider the general idea for realizing our method using a linear optical system. A d -dimensional qudit is encoded in d optical modes of a single photon, which

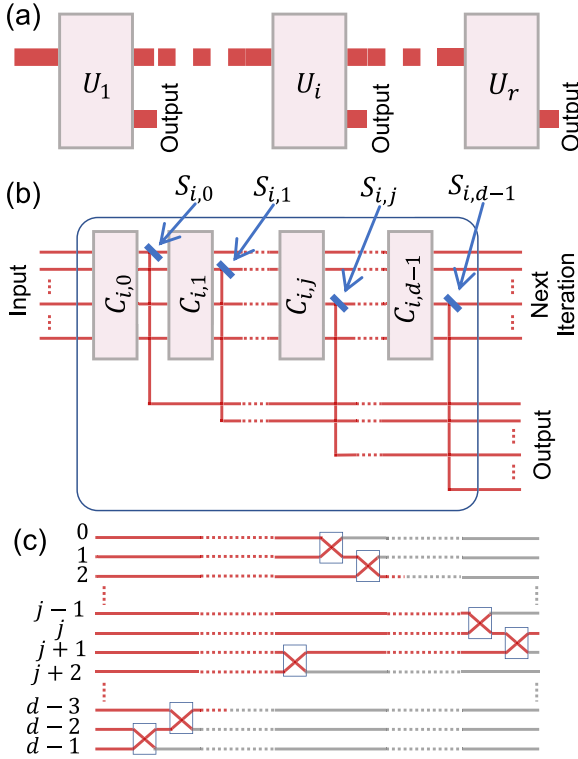


FIG. 3. Illustration of optical realization of our method. (a) The entire optical circuit comprises r unitary operations and r output ports. (b) Each unitary operation U_i can be decomposed into d d -dimensional unitary operations $C_{i,j}$ and d splitters $S_{i,j}$. (c) Each d -dimensional unitary operation $C_{i,j}$ can be achieved through interactions between neighboring modes.

we denoted as $|1, j\rangle$ for $j = 0, \dots, d-1$. To introduce an ancillary qubit, it is easy to use another d mode denoted as $|0, j\rangle$ for $j = 0, \dots, d-1$. In our method, the state of the ancillary qubit before each iteration is $|1\rangle$, meaning that the photon is distributed in the original modes $|1, j\rangle$ as shown in Figs. 3(a) and 3(b). After each transformation U_i , the photon is distributed in $2d$ modes. We output the photon in modes $|0, j\rangle$ while applying the next iteration to the photon in modes $|1, j\rangle$.

The whole process is shown in Fig. 3(a), where there are r output ports. In principle, one can incoherently mix these ports [34] or realize the iterations with loop structures [46]. For simplicity, we realize such a mixture by simultaneously implementing identical operations and measurements on these ports and then discarding the information about in which port the photon is detected.

In our method, each unitary operation U_i is realized by iteratively implementing transformations $A_{i,j}$ and $B_{i,j}$. As shown in Fig. 3(b), each transformation $A_{i,j}$ corresponds to a d -dimensional unitary transformation $C_{i,j}$ on the original modes $|1, j\rangle$ and each transformation $B_{i,j}$ corresponds to a qubit operation $S_{i,j}$ that splits the mode $|1, j\rangle$ into modes $|1, j\rangle$ and $|0, j\rangle$. According to Eq. (6), the transformation $C_{i,j}$ is only required to transform a desired state into $|1, j\rangle$. Therefore, it can be realized by interferences between neighboring modes as shown in Fig. 3(c).

B. Experimental setup for LS channels

We experimentally realize these channels using heralded single photons and linear optical elements (see Fig. 4). Previous experiments in a linear optical system have demonstrated the realization of either TRC [18,21] or TNRC with Kraus rank of 2 [22,23]. Here, our proof-of-principle experiments demonstrate the realization of TNRCs with higher Kraus rank using our method.

In our experiments, a photon pair is generated via type-I spontaneous parametric down-conversion (SPDC) by pumping a 0.5-mm-thick nonlinear β -barium-borate crystal with a 400.8 nm cw diode laser. One of the photons is detected by an avalanche photodiode (APD) to serve as a trigger that heralds the other photon as our single photon source. A qutrit or qudit is encoded in hybrid degrees of freedom (spatial and polarization modes) of the photon. Transformations are realized by optical interferometers in arrays of wave plates (WPs) and polarization-dependent beam displacers (BDs).

The ancillary qubit is encoded in additional spatial modes. Then the operations in step (ii) can be realized as follows. The ancilla-control-system operations $A_{i,j}$ are realized by implementing unitary operations to the original spatial modes while leaving the additional modes unchanged. The system-control-ancilla operations $B_{i,j}$ are realized by partially splitting a photon in an original spatial mode to an additional mode and maintaining the other modes unchanged. The measurement in step (iv) with outcomes 0 or 1 corresponds to finding the photon in these additional or original spatial modes, respectively. After that, the additional spatial modes serve as output ports.

For channels Φ_3 and Φ'_3 , the qutrit bases $|0\rangle, |1\rangle$, and $|2\rangle$ are initially represented by three optical modes, $|P_0V\rangle, |P_1H\rangle$, and $|P_0H\rangle$, where P_i denotes the i th spatial mode and H (V) denotes horizontal (vertical) polarization. In principle, to realize an arbitrary unitary transformation of this photonic qutrit requires three BDs. However, only one row of $C_{i,j}$ is specified, so this transformation can be realized with only two BDs. Moreover, by properly defining the basis and omitting identity operations, the optical circuits are finally simplified to one with only seven BDs as shown in Fig. 4(a). In each output port, the bases of the qutrit states are reencoded by optical modes as $|P_1H\rangle, |P_0H\rangle$, and $|P_0V\rangle$. The changes of the bases can be restored by unitary transformations if necessary.

For the channel Φ_4 , the unitary operations are identical in two subspaces after permutation. Therefore, we use a vertically placed BD (VBD), which transmits the horizontally polarized photon and shifts the vertically polarized photon to a lower mode, to split the photon into two vertically distributed spatial modes denoted as upper $|U\rangle$ and lower $|L\rangle$ modes. The basis of the initial state $|0\rangle, |1\rangle, |2\rangle$, and $|3\rangle$ are encoded by $|LH\rangle, |UH\rangle, |LV\rangle$, and $|UV\rangle$, respectively. The transformations are realized by interferometers with horizontally placed BDs and HWPs, which implement identical operations to upper and lower modes. After phase tuning to the output ports, the basis states of the output are reencoded as $|UV\rangle, |LH\rangle, |UH\rangle$, and $|LV\rangle$. The phase tuning between spatial modes in output ports is realized by tilting the BD in measurement devices when combining the two modes.

As shown in Figs. 4(c) and 4(d), optical circuits for measurements of the qutrit and qudit have the same structure but

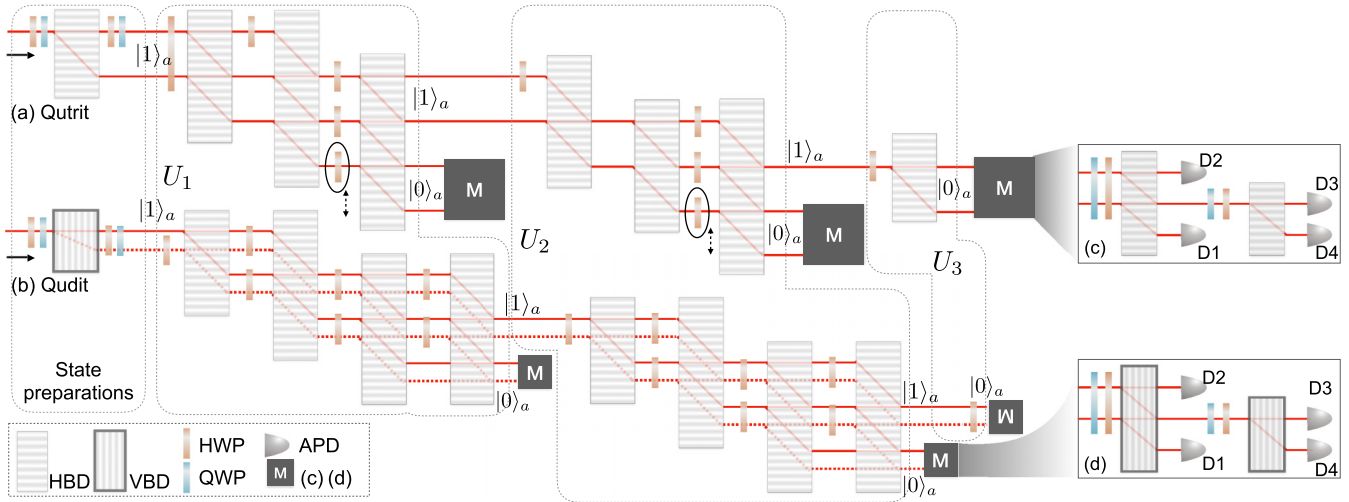


FIG. 4. Optical circuits to realize channels (a) Φ_3 and Φ'_3 (by removing the two HWPs in the ellipses) and (b) Φ_4 . A heralded single photon with horizontal polarization is generated via the spontaneous parametric down-conversion (not shown) and sent to the circuits. The photon is prepared in qutrit or qudit states encoded in hybrid optical modes. Then the photon is iteratively transformed by unitary operations U_1 , U_2 , and U_3 , which are realized by optical interferometers, each with an output port. For each input or output port, the state of the ancillary qubit is labeled as $|0\rangle_a$ or $|1\rangle_a$. Each photon is detected in one and only one of the three output ports. In these ports, we implement the same measurements to act as mixing them. The setups for measurements of qutrit and qudit are shown in (c) and (d), respectively. The third measurement in (b) is marked upside down to indicate that it is implemented in an opposite direction to eliminate a swap operation of spatial modes. HWP: half wave plate; QWP: quarter wave plate.

with BDs being placed in different directions. We adopt this setup to improve the stability of the circuit via sharing the same WPs by two spatial modes. Therefore, the circuit realizes projective measurements (POVM) on the qudit (qutrit) system. The same idea to share WPs is also adopted in the preparation of the qudit state.

All these measurement modules project the photon into four spatial modes, which are finally collected by APDs. In our experiments, we only record the clicks in coincidence with the trigger with a coincident window of 3 ns. Over the exposure time of 10 s, the total coincidence counts are about 1.1×10^5 .

V. EXPERIMENTAL RESULTS

To determine the performance of our experiments, we implement quantum process tomography [47,48] to reconstruct the experimental channels. The reconstructed Choi matrix of experimental channels is shown in Fig. 5. We have calculated the fidelities between these experimental channels Υ^{expt} versus the corresponding intended one Υ^{theor} . In our experiment, the channels Φ_3 , Φ_4 , and Φ'_3 are realized with fidelities 0.9810(9), 0.9509(11), and 0.9831(6), respectively.

To quantify the agreement of a channel Υ^{expt} with UC, we calculate the fidelity between states $\mathbb{1}/d$ and $\Upsilon^{\text{expt}}(\mathbb{1}/d)$ as $\mathcal{F}_{\text{UC}} = \sqrt{\langle \mathbb{1}/d | \Upsilon^{\text{expt}}(\mathbb{1}/d) | \mathbb{1}/d \rangle}$. For channels Φ_3 , Φ_4 , and Φ'_3 , the experimental values of \mathcal{F}_{UC} are 0.999976(6), 0.999960(7), and 0.97709(95), respectively. These results agree with theoretical predictions that Φ_3 and Φ_4 are UC with $\mathcal{F}_{\text{UC}} = 1$ and Φ'_3 is nonunital with $\mathcal{F}_{\text{UC}} = (2 + \sqrt{2} + \sqrt{6})/6 \approx 0.977284$. Here, the accuracies for Φ_3 and Φ_4 are surprisingly good. We conjecture that this occurs because the noise typically present in experiments causes the quantum state to degenerate into a maximally mixed state, which

coincides precisely with the final state of a maximally mixed state after undergoing a UC.

An interesting feature of LSC Φ_d is that it is globally unitarily covariant if and only if $d = 3$ [45]. A channel Φ is globally unitarily covariant if there exists a unitary operation V such that for an arbitrary unitary operation U the equality $\Phi[U\rho U^\dagger] = V\Phi[\rho]V^\dagger$ holds for all states ρ [49]. This strict definition is difficult to satisfy by experimental channels. However, one can estimate a feature implied by the globally unitarily covariant; that is, the final states of such channels $\Phi[U|\psi\rangle\langle\psi|U^\dagger]$ and $\Phi[|\psi\rangle\langle\psi|]$ have identical

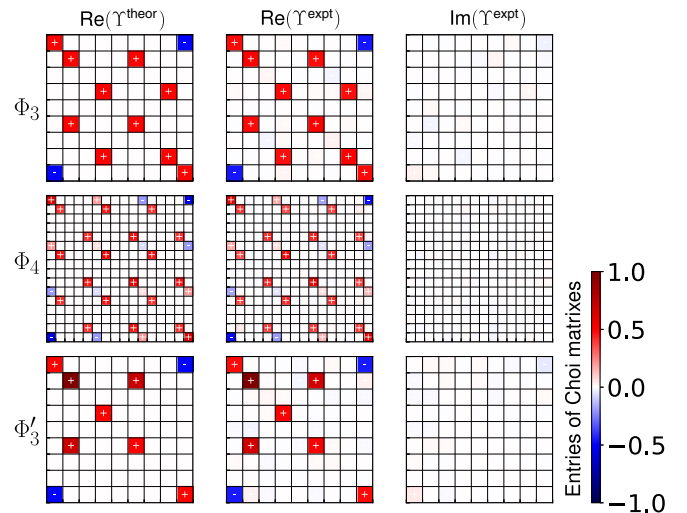


FIG. 5. Theoretical (first column) and experimental (second and third columns) Choi matrices of channels Φ_3 (upper layer), Φ_4 (middle layer), and Φ'_3 (lower layer). The imaginary parts of theoretical Choi matrices are all zero.

spectra for arbitrary U and $|\psi\rangle$. Therefore, these channels induce decoherence to pure states with a state-independent strength.

To quantify the discrepancy between spectra of two states ρ_1 and ρ_2 , we adopt the Jensen-Shannon (JS) distance [50] between two distributions as $D_{\text{JS}}[\text{Spec}(\rho_1), \text{Spec}(\rho_2)]$, where $\text{Spec}(\rho_i)$ denotes the list of eigenvalues of ρ_i sorted from largest to smallest. Here, the JS distance $D_{\text{JS}}(P, Q)$ is a statistical metric for measuring the similarity between two probability distributions P and Q with the same length d as

$$D_{\text{JS}}(P, Q) = \sqrt{\frac{D_{\text{KL}}(P, M) + D_{\text{KL}}(Q, M)}{2}}, \quad (13)$$

where $M = (P + Q)/2$ and $D_{\text{KL}}(P, Q) = \sum_{x=1}^d P_x \log_2 \frac{P_x}{Q_x}$ is the Kullback-Leibler divergence. The JS distance ranges from 0 for identical distributions to 1 for perfect mismatch. For a channel Φ , the maximal divergence is

$$D(\Phi) = \max_{|\psi_1\rangle, |\psi_2\rangle} D_{\text{JS}}(\text{Spec}(\Phi[|\psi_1\rangle\langle\psi_1|]), \text{Spec}(\Phi[|\psi_2\rangle\langle\psi_2|])).$$

Using the reconstructed Choi matrix, the maximal divergences for $\Upsilon_{\Phi_3}^{\text{expt}}$ and $\Upsilon_{\Phi_4}^{\text{expt}}$ are 0.0134(27) and 0.1322(41), respectively. These indicate that the decoherence by $\Upsilon_{\Phi_4}^{\text{expt}}$ is more state dependent than that by $\Upsilon_{\Phi_3}^{\text{expt}}$, which agrees with the theoretical prediction with $D(\Phi_3) = 0$ and $D(\Phi_4) = 0.1258$. Besides, we can roughly estimate the divergences to circumvent the maximization via comparing spectra of the final states obtained in quantum processing tomography. Among these, the largest distances for three- and four-dimensional cases are 0.0140(14) and 0.1107(141), respectively, which also support the decoherence by $\Upsilon_{\Phi_4}^{\text{expt}}$ being more state dependent.

VI. CONCLUSION AND DISCUSSION

In summary, we have proposed a general method to deterministically realize arbitrary TC. This method is simple with parameters determined in an algorithmic way instead of purification of the problem. The method requires only one ancillary qubit and classical controls. Note that the method of randomly implementing operations also requires a qubit when

realizing TNRC, since realizing each nonunitary evolution requires a qubit [28]. Therefore, our method is very efficient in using quantum resources. Moreover, the simulator is in a versatile form of a “digital” one, where unitary evolution can be realized by a sequence of quantum gates [2,21,51,52]. We also experimentally demonstrate the method in realization of both unital and nonunital channels. Our results shed light on quantum simulation of quantum channels for open systems and pave the way for further experimental investigations of quantum channels.

It is worth mentioning that our experimental setup is applicable for adopting other forms of the LV method in a linear optical system. To use our method and other forms of the LV method, it is necessary to have the ability to reuse the postmeasurement state of the ancillary qubit. Otherwise, one should reinitialize the ancillary qubit at each iteration. In this paper, we have demonstrated the method for realizing the ancillary qubit and reusing its postmeasurement state in linear optical systems.

Our method is based on the Kraus representation of a quantum channel and the number of iterations is exactly the Kraus rank. The Kraus representation of a channel with minimum Kraus rank can be obtained from other representation via various procedures [6,38,53,54]. It is worth mentioning that the minimum Kraus rank of a channel of a d -dimensional system is no larger than d^2 [38].

Though our method is proposed for TC, it is also applicable to trace-nonincreasing channels [15] by using partial iterations of realizing a TC. Moreover, the iterations from $(i, j) = (1, 0)$ to $(1, d - 1)$ provide a general, simple, and efficient method for realizing arbitrary nonunitary evolution [29,55]. Considering the similarity between implementing channels and implementing POVM [37,56], our method can also be used to implement POVMs. By implementing projective measurements $|j\rangle\langle j|$ on the system and considering the iteration number i , the POVM elements $|\psi_{i,j}\rangle\langle\psi_{i,j}|$ are realized.

ACKNOWLEDGMENT

This work is supported by the National Natural Science Foundation of China (Grants No. 92265209, No. 12025401, and No. 12004184).

APPENDIX A: OPERATIONS FOR REALIZING Φ_3 , Φ_3' , AND Φ_4 CHANNELS

A choice of $C_{i,j}$ and $r_{i,j}$ for realizing the Φ_3 channel is

$$\begin{aligned} C_{1,0} &= \begin{pmatrix} \sigma_x & \\ & 1 \end{pmatrix}, & C_{1,1} &= \begin{pmatrix} 1 & \\ & H \end{pmatrix}, & C_{1,2} &= \begin{pmatrix} & \sigma_x \\ 1 & \end{pmatrix}, \\ C_{2,0} &= \begin{pmatrix} & -\sigma_x \\ 1 & \end{pmatrix}, & C_{2,1} &= \begin{pmatrix} 1 & \\ & \sigma_x \end{pmatrix}, & C_{2,2} &= \begin{pmatrix} & 1 \\ -\sigma_x & \end{pmatrix}, \\ C_{3,0} &= \begin{pmatrix} -H & \\ & 1 \end{pmatrix}, & C_{3,1} &= \mathbb{1}, & C_{3,2} &= \begin{pmatrix} 1 & \\ & -\sigma_x \end{pmatrix}, \end{aligned}$$

where H denotes the Hadamard gate and

$$r_{1,0} = \frac{1}{2}, \quad r_{1,1} = \frac{1}{\sqrt{2}}, \quad r_{1,2} = \frac{1}{\sqrt{3}}, \quad r_{2,0} = r_{2,1} = \frac{1}{\sqrt{2}}, \quad r_{2,2} = r_{3,0} = r_{3,2} = 1, \quad r_{3,1} = 0.$$

A choice of $C_{i,j}$ and $r_{i,j}$ for realizing the Φ'_3 channel is

$$\begin{aligned} C_{1,0} &= \begin{pmatrix} \sigma_x & \\ & 1 \end{pmatrix}, & C_{1,1} &= \begin{pmatrix} 1 & \\ & H \end{pmatrix}, & C_{1,2} &= \mathbb{1}, \\ C_{2,0} &= \mathbb{1}, & C_{2,1} &= \begin{pmatrix} 1 & \\ & \sigma_x \end{pmatrix}, & C_{2,2} &= \begin{pmatrix} & 1 \\ -\sigma_x & \end{pmatrix}, \\ C_{3,0} &= \begin{pmatrix} H' & \\ & 1 \end{pmatrix}, & C_{3,1} &= \mathbb{1}, & C_{3,2} &= \begin{pmatrix} 1 & \\ & -\sigma_x \end{pmatrix}, \end{aligned}$$

where $H' = (\begin{smallmatrix} 1 & \\ & 1 \end{smallmatrix})/\sqrt{2}$, and

$$r_{1,0} = r_{1,1} = r_{2,1} = \frac{1}{\sqrt{2}}, \quad r_{1,2} = r_{2,2} = r_{3,1} = 0, \quad r_{2,0} = r_{3,0} = r_{3,2} = 1.$$

To simplify the realization of the Φ_4 channel, one can first implement a permutation as

$$P_0 = \begin{pmatrix} & 1 & \\ & & 1 \\ 1 & & \end{pmatrix}.$$

Then one can simplify the procedure by simultaneously implementing transformations to two subspaces, after which permutation and phase tuning should be added to each output. One can realize the procedure with two iterations of j for each i ; that is, for each $j = 0, 1$, one implements $B_{i,j}A_{i,j}$, where

$$A_{i,j} = |1\rangle\langle 1| \otimes \mathbb{1} \otimes C_{i,j} + |0\rangle\langle 0| \otimes \mathbb{1}, \quad B_{i,j} = (r_{i,j}\sigma_x - t_{i,j}\sigma_z) \otimes \mathbb{1} \otimes |j\rangle\langle j| + \mathbb{1} \otimes (\mathbb{1} - \mathbb{1} \otimes |j\rangle\langle j|).$$

Here the operations can be chosen as

$$\begin{aligned} C_{1,0} &= \mathbb{1}, & C_{1,1} &= \begin{pmatrix} -\sqrt{\frac{3}{8}} & \sqrt{\frac{5}{8}} \\ \sqrt{\frac{5}{8}} & \sqrt{\frac{3}{8}} \end{pmatrix}, \\ C_{2,0} &= \begin{pmatrix} -\sqrt{\frac{7}{32}} & \sqrt{\frac{25}{32}} \\ \sqrt{\frac{25}{32}} & \sqrt{\frac{7}{32}} \end{pmatrix}, & C_{2,1} &= \begin{pmatrix} \sqrt{\frac{4}{13}} & \sqrt{\frac{9}{13}} \\ \sqrt{\frac{9}{13}} & -\sqrt{\frac{4}{13}} \end{pmatrix}, \\ C_{3,0} &= \begin{pmatrix} \sqrt{\frac{1}{13}} & \sqrt{\frac{12}{13}} \\ \sqrt{\frac{12}{13}} & -\sqrt{\frac{1}{13}} \end{pmatrix}, & C_{3,1} &= \sigma_z, \end{aligned}$$

and

$$r_{1,0} = \frac{1}{\sqrt{5}}, \quad r_{1,1} = \sqrt{\frac{8}{15}}, \quad r_{2,0} = \sqrt{\frac{3}{7}}, \quad r_{2,1} = \frac{\sqrt{13}}{4}, \quad r_{3,0} = r_{3,1} = 1.$$

If the procedure stops with i , an additional operation PH_i should be implemented to the output, where

$$PH_1 = \begin{pmatrix} 1 & & \\ & 1 & \\ & & 1 \end{pmatrix}, \quad PH_2 = \begin{pmatrix} -1 & & \\ & 1 & \\ & & -1 \end{pmatrix}, \quad PH_3 = \begin{pmatrix} & & -1 \\ 1 & & \\ & 1 & -1 \end{pmatrix}.$$

APPENDIX B: STATE PREPARATIONS AND MEASUREMENTS FOR QUANTUM PROCESS TOMOGRAPHY

In quantum process tomography, we choose states and measurements that are suitable for our setup. For the channel Φ_3 , we prepare the qutrit system in nine states as

$$\begin{pmatrix} 0 \\ 1 \\ 0 \end{pmatrix}, \begin{pmatrix} \frac{1}{\sqrt{2}} \\ \frac{1}{\sqrt{2}} \\ 0 \end{pmatrix}, \begin{pmatrix} \frac{-i}{\sqrt{2}} \\ \frac{1}{\sqrt{2}} \\ 0 \end{pmatrix}, \begin{pmatrix} 0 \\ \frac{1}{\sqrt{2}} \\ \frac{1}{\sqrt{2}} \end{pmatrix}, \\ \begin{pmatrix} 0 \\ \frac{1}{\sqrt{2}} \\ \frac{i}{\sqrt{2}} \end{pmatrix}, \begin{pmatrix} 0 \\ 0 \\ 1 \end{pmatrix}, \begin{pmatrix} 1 \\ 0 \\ 0 \end{pmatrix}, \begin{pmatrix} \frac{1}{\sqrt{2}} \\ 0 \\ \frac{i}{\sqrt{2}} \end{pmatrix}, \begin{pmatrix} \frac{1}{\sqrt{2}} \\ 0 \\ \frac{-1}{\sqrt{2}} \end{pmatrix}.$$

The measurements are POVMs $\{|m_k\rangle\langle m_k|, \mathbb{1} - |m_k\rangle\langle m_k|\}$, where the element $|m_k\rangle\langle m_k|$ corresponds to APD D3 and $|m_k\rangle$ are chosen as follows:

$$\begin{pmatrix} 0 \\ 1 \\ 0 \end{pmatrix}, \begin{pmatrix} 0 \\ \frac{1}{\sqrt{2}} \\ \frac{-i}{\sqrt{2}} \end{pmatrix}, \begin{pmatrix} 0 \\ \frac{1}{\sqrt{2}} \\ \frac{1}{\sqrt{2}} \end{pmatrix}, \begin{pmatrix} -1/2 \\ 1/2 \\ 1/2 \end{pmatrix}, \\ \begin{pmatrix} -i/2 \\ 1/2 \\ -i/2 \end{pmatrix}, \begin{pmatrix} 1 \\ 0 \\ 0 \end{pmatrix}, \begin{pmatrix} 0 \\ 0 \\ 1 \end{pmatrix}, \begin{pmatrix} \frac{1}{\sqrt{2}} \\ 0 \\ \frac{1}{\sqrt{2}} \end{pmatrix}, \begin{pmatrix} \frac{1}{\sqrt{2}} \\ 0 \\ \frac{-i}{\sqrt{2}} \end{pmatrix}.$$

For the channel Φ_4 , the qudit system is prepared in 16 states as

$$\begin{pmatrix} 0 \\ 1 \\ 0 \\ 0 \end{pmatrix}, \begin{pmatrix} 0 \\ 0 \\ 0 \\ 1 \end{pmatrix}, \begin{pmatrix} 0 \\ \frac{1}{\sqrt{2}} \\ 0 \\ \frac{i}{\sqrt{2}} \end{pmatrix}, \begin{pmatrix} 0 \\ \frac{1}{\sqrt{2}} \\ 0 \\ \frac{1}{\sqrt{2}} \end{pmatrix}, \begin{pmatrix} \frac{-1}{\sqrt{2}} \\ 0 \\ \frac{1}{\sqrt{2}} \\ 0 \end{pmatrix}, \begin{pmatrix} \frac{i}{\sqrt{2}} \\ 0 \\ \frac{1}{\sqrt{2}} \\ 0 \end{pmatrix}, \\ \begin{pmatrix} 1 \\ 0 \\ 0 \\ 0 \end{pmatrix}, \begin{pmatrix} 0 \\ 0 \\ 1 \\ 0 \end{pmatrix}, \begin{pmatrix} 0 \\ \frac{1}{\sqrt{2}} \\ \frac{1}{\sqrt{2}} \\ 0 \end{pmatrix}, \begin{pmatrix} \frac{1}{\sqrt{2}} \\ 0 \\ 0 \\ \frac{1}{\sqrt{2}} \end{pmatrix}, \begin{pmatrix} i/2 \\ 1/2 \\ 1/2 \\ i/2 \end{pmatrix}, \begin{pmatrix} -1/2 \\ 1/2 \\ 1/2 \\ 1/2 \end{pmatrix}, \\ \begin{pmatrix} i/2 \\ 1/2 \\ -i/2 \\ 1/2 \end{pmatrix}, \begin{pmatrix} 1/2 \\ 1/2 \\ -1/2 \\ i/2 \end{pmatrix}, \begin{pmatrix} \frac{1}{\sqrt{2}} \\ 0 \\ 0 \\ \frac{i}{\sqrt{2}} \end{pmatrix}, \begin{pmatrix} 0 \\ \frac{1}{\sqrt{2}} \\ \frac{-i}{\sqrt{2}} \\ 0 \end{pmatrix}.$$

The measurement corresponding to APD D3 is projective measurement $|m_i\rangle\langle m_i|$ with the 16 $|m_i\rangle$ as

$$\begin{pmatrix} 0 \\ 1 \\ 0 \\ 0 \end{pmatrix}, \begin{pmatrix} 0 \\ 0 \\ 0 \\ 1 \end{pmatrix}, \begin{pmatrix} 0 \\ \frac{1}{\sqrt{2}} \\ 0 \\ \frac{-i}{\sqrt{2}} \end{pmatrix}, \begin{pmatrix} 0 \\ \frac{1}{\sqrt{2}} \\ 0 \\ \frac{1}{\sqrt{2}} \end{pmatrix}, \begin{pmatrix} \frac{1}{\sqrt{2}} \\ 0 \\ \frac{-1}{\sqrt{2}} \\ 0 \end{pmatrix}, \begin{pmatrix} \frac{1}{\sqrt{2}} \\ 0 \\ \frac{-i}{\sqrt{2}} \\ 0 \end{pmatrix}, \\ \begin{pmatrix} 0 \\ 0 \\ 1 \\ 0 \end{pmatrix}, \begin{pmatrix} 1 \\ 0 \\ 0 \\ 0 \end{pmatrix}, \begin{pmatrix} \frac{1}{\sqrt{2}} \\ \frac{1}{\sqrt{2}} \\ 0 \\ 0 \end{pmatrix}, \begin{pmatrix} 0 \\ 0 \\ \frac{1}{\sqrt{2}} \\ \frac{1}{\sqrt{2}} \end{pmatrix}, \begin{pmatrix} 1/2 \\ 1/2 \\ -i/2 \\ -i/2 \end{pmatrix}, \begin{pmatrix} 1/2 \\ 1/2 \\ -1/2 \\ -1/2 \end{pmatrix}, \\ \begin{pmatrix} i/2 \\ 1/2 \\ -i/2 \\ 1/2 \end{pmatrix}, \begin{pmatrix} i/2 \\ 1/2 \\ 1/2 \\ -i/2 \end{pmatrix}, \begin{pmatrix} 0 \\ 0 \\ \frac{1}{\sqrt{2}} \\ \frac{-i}{\sqrt{2}} \end{pmatrix}, \begin{pmatrix} 0 \\ \frac{1}{\sqrt{2}} \\ \frac{1}{\sqrt{2}} \\ 0 \end{pmatrix}.$$

- [1] R. P. Feynman, Simulating physics with computers, *Int. J. Theor. Phys.* **21**, 467 (1982).
- [2] I. Buluta and F. Nori, Quantum simulators, *Science* **326**, 108 (2009).
- [3] K. L. Brown, W. J. Munro, and V. M. Kendon, Using quantum computers for quantum simulation, *Entropy* **12**, 2268 (2010).
- [4] I. M. Georgescu, S. Ashhab, and F. Nori, Quantum simulation, *Rev. Mod. Phys.* **86**, 153 (2014).
- [5] A. M. Childs, D. Maslov, Y. Nam, N. J. Ross, and Y. Su, Toward the first quantum simulation with quantum speedup, *Proc. Natl. Acad. Sci. USA* **115**, 9456 (2018).
- [6] M. A. Nielsen and I. L. Chuang, *Quantum Computation and Quantum Information* (Cambridge University Press, Cambridge, UK, 2010).
- [7] A. Cuevas, M. Proietti, M. A. Ciampini, S. Duranti, P. Mataloni, M. F. Sacchi, and C. Macchiavello, Experimental Detection of Quantum Channel Capacities, *Phys. Rev. Lett.* **119**, 100502 (2017).
- [8] V. Cimini, I. Gianani, M. F. Sacchi, C. Macchiavello, and M. Barbieri, Experimental witnessing of the quantum channel capacity in the presence of correlated noise, *Phys. Rev. A* **102**, 052404 (2020).
- [9] B. Regula and R. Takagi, Fundamental limitations on distillation of quantum channel resources, *Nat. Commun.* **12**, 4411 (2021).
- [10] X. Zhan, D. Qu, K. Wang, L. Xiao, and P. Xue, Experimental detection of qubit-environment entanglement without accessing the environment, *Phys. Rev. A* **104**, L020201 (2021).
- [11] J. Fiurášek, Extremal equation for optimal completely positive maps, *Phys. Rev. A* **64**, 062310 (2001).
- [12] K. Bartkiewicz, K. Lemr, A. Černoch, J. Soubusta, and A. Miranowicz, Experimental Eavesdropping Based on Optimal Quantum Cloning, *Phys. Rev. Lett.* **110**, 173601 (2013).
- [13] K. Bartkiewicz, A. Černoch, G. Chimczak, K. Lemr, A. Miranowicz, and F. Nori, Experimental quantum forgery of quantum optical money, *npj Quantum Inf.* **3**, 7 (2017).
- [14] W. F. Stinespring, Positive functions on c^* -algebras, *Proc. Am. Math. Soc.* **6**, 211 (1955).
- [15] D.-S. Wang, D. W. Berry, M. C. de Oliveira, and B. C. Sanders, Solovay-Kitaev Decomposition Strategy for Single-Qubit Channels, *Phys. Rev. Lett.* **111**, 130504 (2013).
- [16] S.-J. Wei, T. Xin, and G.-L. Long, Efficient universal quantum channel simulation in IBM's cloud quantum computer, *Sci. China Phys. Mech.* **61**, 70311 (2018).
- [17] M. Ricci, F. De Martini, N. J. Cerf, R. Filip, J. Fiurášek, and C. Macchiavello, Experimental Purification of Single Qubits, *Phys. Rev. Lett.* **93**, 170501 (2004).
- [18] A. Chiuri, V. Rosati, G. Vallone, S. Pádua, H. Imai, S. Giacomini, C. Macchiavello, and P. Mataloni, Experimental Realization of Optimal Noise Estimation for a General Pauli Channel, *Phys. Rev. Lett.* **107**, 253602 (2011).
- [19] A. Shaham and H. S. Eisenberg, Realizing controllable depolarization in photonic quantum-information channels, *Phys. Rev. A* **83**, 022303 (2011).
- [20] A. Orioux, L. Sansoni, M. Persechini, P. Mataloni, M. Rossi, and C. Macchiavello, Experimental Detection of Quantum Channels, *Phys. Rev. Lett.* **111**, 220501 (2013).
- [21] H. Lu, C. Liu, D.-S. Wang, L.-K. Chen, Z.-D. Li, X.-C. Yao, L. Li, N.-L. Liu, C.-Z. Peng, B. C. Sanders, Y.-A. Chen, and J.-W. Pan, Experimental quantum channel simulation, *Phys. Rev. A* **95**, 042310 (2017).
- [22] Y.-S. Kim, J.-C. Lee, O. Kwon, and Y.-H. Kim, Protecting entanglement from decoherence using weak measurement and quantum measurement reversal, *Nat. Phys.* **8**, 117 (2012).
- [23] K. Wang, X. Wang, X. Zhan, Z. Bian, J. Li, B. C. Sanders, and P. Xue, Entanglement-enhanced quantum metrology in a noisy environment, *Phys. Rev. A* **97**, 042112 (2018).
- [24] J.-C. Lee, Y.-C. Jeong, Y.-S. Kim, and Y.-H. Kim, Experimental demonstration of decoherence suppression via quantum measurement reversal, *Opt. Express* **19**, 16309 (2011).
- [25] K. A. G. Fisher, R. Prevedel, R. Kaltenbaek, and K. J. Resch, Optimal linear optical implementation of a single-qubit damping channel, *New J. Phys.* **14**, 033016 (2012).
- [26] A. Orioux, M. A. Ciampini, P. Mataloni, D. Bruß, M. Rossi, and C. Macchiavello, Experimental Generation of Robust Entanglement from Classical Correlations via Local Dissipation, *Phys. Rev. Lett.* **115**, 160503 (2015).
- [27] C.-Y. Ju, A. Miranowicz, G.-Y. Chen, and F. Nori, Non-Hermitian Hamiltonians and no-go theorems in quantum information, *Phys. Rev. A* **100**, 062118 (2019).
- [28] K. Kawabata, Y. Ashida, and M. Ueda, Information Retrieval and Criticality in Parity-Time-Symmetric Systems, *Phys. Rev. Lett.* **119**, 190401 (2017).
- [29] L. Xiao, K. Wang, X. Zhan, Z. Bian, K. Kawabata, M. Ueda, W. Yi, and P. Xue, Observation of Critical Phenomena in Parity-Time-Symmetric Quantum Dynamics, *Phys. Rev. Lett.* **123**, 230401 (2019).
- [30] Y.-C. Lee, M.-H. Hsieh, S. T. Flammia, and R.-K. Lee, Local \mathcal{PT} Symmetry Violates the No-Signaling Principle, *Phys. Rev. Lett.* **112**, 130404 (2014).
- [31] J.-S. Tang, Y.-T. Wang, S. Yu, D.-Y. He, J.-S. Xu, B.-H. Liu, G. Chen, Y.-N. Sun, K. Sun, Y.-J. Han, C.-F. Li, and G.-C. Guo, Experimental investigation of the no-signalling principle in parity-time symmetric theory using an open quantum system, *Nat. Photon.* **10**, 642 (2016).
- [32] X. Zhan, K. Wang, L. Xiao, Z. Bian, Y. Zhang, B. C. Sanders, C. Zhang, and P. Xue, Experimental quantum cloning in a pseudo-unitary system, *Phys. Rev. A* **101**, 010302(R) (2020).
- [33] S. Lloyd and L. Viola, Engineering quantum dynamics, *Phys. Rev. A* **65**, 010101(R) (2001).
- [34] M. P. Almeida, F. de Melo, M. Hor-Meyll, A. Salles, S. P. Walborn, P. H. S. Ribeiro, and L. Davidovich, Environment-induced sudden death of entanglement, *Science* **316**, 579 (2007).
- [35] J.-S. Xu, C.-F. Li, M. Gong, X.-B. Zou, C.-H. Shi, G. Chen, and G.-C. Guo, Experimental Demonstration of Photonic Entanglement Collapse and Revival, *Phys. Rev. Lett.* **104**, 100502 (2010).
- [36] C. Shen, K. Noh, V. V. Albert, S. Krastanov, M. H. Devoret, R. J. Schoelkopf, S. M. Girvin, and L. Jiang, Quantum channel construction with circuit quantum electrodynamics, *Phys. Rev. B* **95**, 134501 (2017).
- [37] E. Andersson and D. K. L. Oi, Binary search trees for generalized measurements, *Phys. Rev. A* **77**, 052104 (2008).
- [38] M.-D. Choi, Completely positive linear maps on complex matrices, *Linear Algebra Appl.* **10**, 285 (1975).

- [39] A. Jamiołkowski, Linear transformations which preserve trace and positive semidefiniteness of operators, *Rep. Math. Phys.* **3**, 275 (1972).
- [40] S. Milz, F. A. Pollock, and K. Modi, An introduction to operational quantum dynamics, *Open Syst. Inf. Dyn.* **24**, 1740016 (2017).
- [41] M. Raginsky, A fidelity measure for quantum channels, *Phys. Lett. A* **290**, 11 (2001).
- [42] R. Penrose, A generalized inverse for matrices, in *Mathematical Proceedings of the Cambridge Philosophical Society* (Cambridge University Press, Cambridge, UK, 1955), Vol. 51, pp. 406–413.
- [43] Z. Li, H. Zhang, and H. Zhu, Implementation of generalized measurements on a qudit via quantum walks, *Phys. Rev. A* **99**, 062342 (2019).
- [44] L. J. Landau and R. F. Streater, On Birkhoff’s theorem for doubly stochastic completely positive maps of matrix algebras, *Linear Algebra Appl.* **193**, 107 (1993).
- [45] S. N. Filippov and K. V. Kuzhamuratova, Quantum informational properties of the Landau–Streater channel, *J. Math. Phys.* **60**, 042202 (2019).
- [46] K. Bartkiewicz, A. Černoč, K. Lemr, A. Miranowicz, and F. Nori, Experimental temporal quantum steering, *Sci. Rep.* **6**, 38076 (2016).
- [47] J. L. O’Brien, G. J. Pryde, A. Gilchrist, D. F. V. James, N. K. Langford, T. C. Ralph, and A. G. White, Quantum Process Tomography of a Controlled-NOT Gate, *Phys. Rev. Lett.* **93**, 080502 (2004).
- [48] D. F. V. James, P. G. Kwiat, W. J. Munro, and A. G. White, Measurement of qubits, *Phys. Rev. A* **64**, 052312 (2001).
- [49] A. S. Holevo, Covariant quantum markovian evolutions, *J. Math. Phys.* **37**, 1812 (1996).
- [50] B. Fuglede and F. Topsøe, Jensen-Shannon divergence and Hilbert space embedding, in *Proceedings of the International Symposium on Information Theory, 2004* (IEEE, New York, 2004), p. 31.
- [51] L. M. Sieberer, T. Olsacher, A. Elben, M. Heyl, P. Hauke, F. Haake, and P. Zoller, Digital quantum simulation, trotter errors, and quantum chaos of the kicked top, *npj Quantum Inf.* **5**, 78 (2019).
- [52] J. I. Cirac and P. Zoller, Goals and opportunities in quantum simulation, *Nat. Phys.* **8**, 264 (2012).
- [53] J. Watrous, *The Theory of Quantum Information* (Cambridge University Press, Cambridge, UK, 2018).
- [54] M. M. Wilde, *Quantum Information Theory*, 2nd ed. (Cambridge University Press, Cambridge, UK, 2017).
- [55] U. Günther and B. F. Samsonov, Naimark-Dilated PT-Symmetric Brachistochrone, *Phys. Rev. Lett.* **101**, 230404 (2008).
- [56] G. Wang and M. Ying, Realization of positive-operator-valued measures by projective measurements without introducing ancillary dimensions, [arXiv:quant-ph/0608235](https://arxiv.org/abs/quant-ph/0608235).